Runaway and Moist Greenhouse Atmospheres and the Evolution of Earth and Venus

JAMES F. KASTING

Space Science Division 245-3, NASA Ames Research Center, Moffett Field, California 94035

A one-dimensional climate model is used to study the response of an Earth-like atmosphere to large increases in solar flux. For fully saturated, cloud-free conditions, the critical solar flux at which a runaway greenhouse occurs, that is, the oceans evaporate entirely, is found to be 1.4 times the present flux at Earth's orbit (S_o). This value is close to the flux expected at Venus' orbit early in solar system history. It is nearly independent of the amount of CO_2 present in the atmosphere, but is sensitive to the H_2O absorption coefficient in the 8- to 12-μm window region. Clouds should tend to depress the surface temperature on a warm, moist planet; thus, Venus may originally have had oceans if its initial water endowment was close to that of Earth. It lost them early in its history, however, because of rapid photodissociation of water vapor followed by escape of hydrogen to space. The critical solar flux above which water is rapidly lost could be as low as $1.1S_o$. The surface temperature of a runaway greenhouse atmosphere containing a full ocean's worth of water would have been in excess of 1500°K—above the solidus for silicate rocks. The presence of such a steam atmosphere during accretion may have significantly influenced the early thermal evolution of both Earth and Venus. © 1988 Academic Press, Inc.

1. INTRODUCTION

The question of how Earth's surface temperature would respond to an increase in solar flux is intriguing from a purely academic standpoint and is also relevant to understanding why the atmosphere of Venus is so different from that of Earth. Several recent investigations of this problem (Lindzen *et al.* 1982, Kasting *et al.* 1984, Vardavas and Carver 1985) have come to markedly different conclusions. Lindzen *et al.* challenged the idea, originally suggested by Ingersoll (1969), that increased solar heating would eventually lead to a runaway greenhouse, that is, to complete evaporation of the oceans. Lindzen *et al.* argued (correctly) that the effect of moist convection on the tropospheric lapse rate provides a strong stabilizing influence on surface temperature. They even went so far as to suggest that there is an asymptotic upper

limit on surface temperature ($T_s = 41$°C), which cannot be exceeded even for very large (factor of 2) solar flux increases. Their model was criticized in several subsequent studies, including Lal and Ramanathan (1984), Kasting *et al.* (1984) (henceforth, KPA), and Vardavas and Carver (1985). All of these investigators agreed that the upper limit on T_s calculated by Lindzen *et al.* was unrealistic. The fundamental problem was their use of water vapor emissivities exceeding unity, which caused their model atmosphere to radiate more efficiently than a blackbody (Vardavas and Carver 1985). KPA pointed out that surface temperatures in the Lindzen *et al.* model should also have been suppressed by their adoption of the empirical relative humidity profile of Manabe and Wetherald (1967) and by the vanishingly small lapse rate near the surface predicted by their "cumulus" model for convection.

KPA next performed a similar calculation, assuming a fully saturated troposphere and using the moist adiabatic lapse rate. They predicted that T_s should increase monotonically with increasing solar flux up to at least 1.45 times the present terrestrial value. (Their calculation, like that of Lindzen et al., dealt exclusively with infrared fluxes; a constant planetary albedo was assumed.) Their model did not predict a runaway greenhouse for early Venus either. Instead, KPA suggested that Venus could have had a relatively thin (~2 bar) N_2–H_2O atmosphere with a surface temperature near 100°C. They showed that H_2O would have remained a major constituent of such an atmosphere up to very high altitudes, so that water could have been rapidly lost by photodissociation followed by hydrogen escape. KPA termed this atmosphere a "moist greenhouse" and argued that this model could explain the present aridity and high D/H ratio of Venus as well, or better, than could the runaway greenhouse model.

KPA's conclusions were challenged by a new radiative-convective model study by Vardavas and Carver (1985). Vardavas and Carver pointed out that the lapse rate formulation used by KPA was incorrect. This turns out not to have been a significant source of error; both their formulation and that of KPA give approximately the same lapse rate. A corrected formulation of the moist adiabatic lapse rate is given in Appendix A of this paper. More importantly, however, Vardavas and Carver argued that the planetary albedo should decrease at higher surface temperatures because of increased absorption of solar radiation by atmospheric water vapor. The results of their calculation were strikingly different from those of KPA: For the same fully saturated conditions, they predicted that a runaway greenhouse would ensue for a mere 2% increase in the solar constant S_0 at Earth's orbit. Vardavas and Carver did not actually demonstrate this explicitly; rather, they showed that T_s increases extremely rapidly with solar flux near $1.02S_0$.

In this paper, I reexamine the response of Earth's surface temperature to increases in solar flux. This paper is an extension of previous work by Kasting and Ackerman (1986), who showed that CO_2 increases alone would not trigger a runaway greenhouse. The approach taken in that study was to estimate upper limits on surface temperature at a given CO_2 level. Lower limits on T_s are much more difficult to determine because of uncertainties related to relative humidity and clouds. The philosophy of this paper is similar. My goal is to estimate an upper limit on T_s at a given value of the solar flux. A second goal is to estimate the surface temperature of a runaway greenhouse atmosphere and to compare with previous predictions by Watson et al. (1984) and by Matsui and Abe (1986a,b). Finally, the results of the model are used to speculate about when an Earth-like planet might lose its water and how much closer to the Sun Earth could have formed without ending up like Venus.

2. MODEL DESCRIPTION

(a) Radiative Model

The radiative-convective model used here is derived from the model used by Kasting and Ackerman (1986) to study the response of Earth's surface temperature to large increases in CO_2. It uses a δ two-stream scattering formulation to calculate absorption of solar radiation and employs random band models (Fels/Goody for H_2O, Malkmus for CO_2) to determine the outgoing terrestrial radiation. Continuum absorption by H_2O and pressure-induced absorption by CO_2 are treated differently. The original model divided the infrared spectrum from 0.67 to 500 μm into 55 spectral intervals. Absorption coefficients were derived by fitting synthetic spectra computed from the AFGL tape (McClatchey et al. 1971). In the present model seven additional intervals have been added to cover the visible spectrum down to 0.39 μm. These shorter wavelengths become impor-

tant to the terrestrial radiation budget at surface temperatures above 1400°K. Absorption by H_2O in this spectral region was estimated by the method described in Appendix B. This method predicts substantially less absorption than does the continuum formulation employed by Vardavas and Carver (1985). Absorption by CO_2 between 0.71 and 1.04 μm was estimated from laboratory spectra (Herzberg and Herzberg 1953).

Two features of the radiative model deserve further elaboration because they bear directly on the results. First, and most importantly, H_2O has a finite absorption coefficient in this model in every spectral interval longward of 0.63 μm The same was was not true of the model of KPA. That model utilized near-infrared absorption data from Howard et al. (1956) which covered only the strongest H_2O bands. The absence of absorption gaps in the present model ensures that a sufficiently dense H_2O atmosphere can become optically thick at all infrared wavelengths. This factor is of critical importance in determining whether or not a runaway greenhouse will occur.

Second, the temperature dependence of the band model coefficients (two each for H_2O and for CO_2) was assumed to be given by

$$X(T) = X(300) \ \exp[a(T - 300) + b(T - 300)^2]. \quad (1)$$

Here, $X(300)$ represents the value of the coefficient at 300°K. The values of a and b were determined from additional calculations at 200 and 600°K. In the present model the temperature dependence was extrapolated up to 1000°K, above which point the coefficients were assumed to remain constant. The lack of information about the absorption coefficients at high temperatures makes it impossible to determine accurate radiative fluxes deep within a runaway greenhouse atmosphere. This limitation is not as serious as it might seem because most of the energy transport in this region takes place by convection. Thus,

even relatively large errors in the radiative flux at most wavelengths should have little effect on the calculated energy budget. At some near-infrared wavelengths, however, water vapor is nearly transparent and radiation from the surface can escape directly to space. Here, the uncertainty in the absorption coefficients leads to a corresponding uncertainty in the outgoing radiation flux. This problem is compounded in the visible where the temperature dependence of the band model coefficients is unknown (see Appendix B). The opacity in the 8- to 12-μm region is likewise ill-determined above about 430°K, the highest temperatures studied in the experiments of Burch et al. (1971).

(b) Atmospheric Composition and Relative Humidity

The background atmosphere assumed in most of the calculations was an Earth-like N_2–O_2–CO_2 atmosphere without any O_3. Ozone would presumably be destroyed in a warm, moist atmosphere by the by-products of water vapor photolysis. Sensitivity calculations were performed to determine the effect of higher concentrations of CO_2. The surface pressure was assumed to be given by

$$P_s = 1 + pCO_2 + pH_2O, \quad (2)$$

where pH_2O is the saturation vapor pressure of water at the surface temperature T_s.

The relative humidity within the moist convective region was assumed equal to unity, in accord with my goal of estimating upper limits on T_s. Although this overestimates the amount of water vapor in the upper troposphere of the present Earth, it is a reasonable choice for an atmosphere in which water vapor is a major constituent. In most cases of interest here water vapor is in fact the dominant atmospheric constituent, and the relative humidity could not have fallen much below unity without violating the barometric law. The water vapor mixing ratio in the stratosphere was set

equal to its value at the top of the convective zone.

It should be noted that most conventional 1-D climate modelers, including Lindzen *et al.* (1982), have used the empirical relative humidity profile of Manabe and Wetherald (1967) in their calculations. This assumption is not acceptable if one wishes to understand the evolution of Venus, because it automatically ensures that the upper troposphere and stratosphere will be dry. Venus, on the other hand, could have lost large quantities of water only if its stratosphere was originally wet. Short of actually calculating relative humidity, which would require a multidimensional model, two types of approaches to this problem can be envisioned. The simplest is to assume that the troposphere is completely saturated. The alternative is to adopt a parameterization, such as that used by Kasting and Ackerman (1986), that connects unsaturated solutions at low T_s with highly saturated solutions at high T_s. I have taken the simple approach here, because it produces a true upper limit on surface temperatures and because it is a sensible choice for atmospheres that are dominated by water vapor.

(c) Clouds

Clouds were excluded from most of these calculations because it is not known how they would vary in an atmosphere much hotter (or colder) than our own. Their effect was included implicitly by adopting a high value ($A_s = 0.22$) for the surface albedo. This value of A_s was chosen because it allows the climate model to reproduce the current mean global surface temperature (288°K), given the current solar insolation. This approximation is equivalent to assuming that the cloud layer is at the ground. By holding A_s constant at higher surface temperatures, I assume no cloud feedback whatsoever.

In reality, clouds, could form at a variety of heights in a warm, moist atmosphere, and their effect on T_s should depend on their location. A limited number of numeri-

cal experiments were performed to determine the magnitude of this effect. In these calculations, a single cloud layer consisting of spherical water droplets with a log normal size distribution and a 5-μm mean radius was presumed to be present at various heights within the atmosphere. The thickness of the cloud was taken to be approximately one pressure scale height. The liquid water content (W) of the cloud was assumed to be proportional to the local atmospheric mass density (ρ). This assumption is reasonable if vertical motions within the atmosphere remain roughly equivalent to those today, since the force that suspends the cloud particles is proportional to the product of the vertical wind speed and the local atmospheric density. For typical stratiform clouds on the present Earth, W is equal to ~ 0.5 g m^{-3} and ρ is about 1200 g m^3, so the ratio W/ρ is about 4×10^{-4}. This same ratio was assumed for all clouds in the model.

The scattering properties of the cloud particles were specified by simple numerical formulas that approximate the results of sophisticated Mie calculations. The single scattering albedo ω_0 of the particles was assumed to be equal to 1 for $\lambda < 2$ μm, or 1.24 $\lambda^{-0.32}$ for $\lambda \geq 2$ μm. The asymmetry factor g was set equal to 0.85 for $\lambda < 10$ μm, or 1.40 $\lambda^{-0.22}$ for $\lambda \geq 10$ μm. The extinction efficiency Q_e was set equal to 1 for $\lambda < 20$ μm, or 3.26 $\lambda^{-0.40}$ for $\lambda \geq 20$ μm. The extinction coefficient at 0.55 μm was taken to be 0.13 m^2 g^{-1}. The extinction coefficient at other wavelengths was set equal to this value times Q_e.

(d) Thermal Structure

The present model is similar to the model of Pollack (1971) in that the temperature structure of the atmosphere was assumed rather than calculated. This assumption is motivated primarily by expedience. As discussed by KPA, the Newton–Raphson iteration procedure used in their steady-state radiative-convective model fails to converge at high surface temperatures
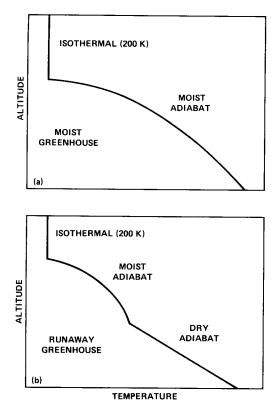
FIG. 1. Schematic diagram of assumed thermal structure for (a) moist and (b) runaway greenhouse atmospheres.

which the lapse rate follows a moist pseudoadiabat, that is, an adiabat in which the condensed phase leaves the system immediately. The mathematical expression for the lapse rate is presented in Appendix A. Here, and throughout the model, water vapor was treated as a nonideal gas. At high surface temperatures the moist convective region was presumed to be underlain by an unsaturated region in which the lapse rate follows a dry adiabat. The lapse rate here is necessarily steeper than in the moist convective region because of the absence of latent heat release from condensation. The boundary between the moist and dry layers was determined by keeping track of the water vapor volume mixing ratio. The H_2O mixing ratio remains constant in the dry convective region; its value there is determined by the total amount of water and background gas assumed to be present. Because the dry adiabatic lapse rate is steeper than the saturation vapor pressure curve, water vapor reaches saturation at some height above the surface. This point marks the top of the dry convective region. Whether or not this unsaturated region should exist in the first place was determined by comparing the saturation vapor pressure at temperature T_s with the total amount of water assumed to be present at the planet's surface.

The actual lapse rate within the convective region may, of course, not have been adiabatic. Various alternative methods for parameterizing the temperature gradients associated with convection have been proposed, ranging from mixing length theory (Mihalas 1978) to the "cumulus" model of Lindzen et al. (1982). The lapse rate at midlatitudes in the Earth's troposphere is also modified by the breaking of baroclinic waves, a dynamical effect that cannot be modeled in one dimension. Without debating the relative merits of the various approaches to convection, let it suffice to say that adopting the adiabatic lapse is both practical and, at the same time, unlikely to lead one too far astray. Wave breaking

($>110°C$) because of the strong coupling between surface temperature and pressure. This problem can apparently be overcome by using a model that adds or subtracts grid points as the surface pressure changes (Y. Abe, private communication, 1987). The present model, on the other hand, is much cheaper to run. Fortunately, it can also be demonstrated (see below) that this assumption results in no significant loss of generality for the results. By contrast, KPA, Watson et al. (1984), and Vardavas and Carver (1985) all calculated temperature profiles self-consistently.

The temperature structure assumed here is shown in Fig. 1. At low surface temperatures the atmosphere was presumed to consist of an isothermal (200°K) stratosphere underlain by a convective troposphere in

tends to decrease the lapse rate and, hence, would only lower surface temperatures relative to those predicted here. Since the temperatures calculated here represent upper limits, this should not in any way compromise the results.

In addition to allowing the calculations to be extended to high surface temperatures, specifying the temperature structure in this manner simplifies the flux calculation enormously. In a standard radiative-convective calculation, a trial temperature profile is assumed, radiative fluxes are evaluated at all levels, and then the temperature profile is adjusted so as to try to achieve flux balance in the stratosphere. This procedure is repeated (either iteratively or in time-marching mode) until the temperature profile is converged. In the present model, no iteration is required. The temperature profile is specified, and the radiative fluxes are evaluated at the top atmospheric level. (Actually, the solar flux calculation must be done at all levels simultaneously because it involves scattering.) The effective solar constant corresponding to a given surface temperature is determined by ratioing the net incoming solar and outgoing infrared fluxes at the top of the atmosphere. A typical flux calculation can be performed in a fraction of a second on a Cray X-MP computer, whereas a standard radiative-convective model calculation can require several minutes of computer time.

Although this procedure may sound overly simplistic it can be demonstrated that the approximations made here have a sound physical basis. To see why this is so it is necessary to jump ahead to some of the results. These will be placed in their proper context in the next section.

Figure 2 shows net upward infrared and net downward solar fluxes for a moist greenhouse atmosphere with a surface temperature of 100°C. The surface pressure of this atmosphere is 2 bar, half of which is attributable to water vapor and the rest to N_2 and O_2. The solar flux shown here is consistent with a solar constant of
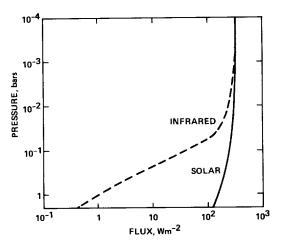

FIG. 2. Net upward infrared (dashed curve) and downward solar (solid curve) fluxes for an Earth-like atmosphere with a surface temperature of 100°C. The total incident solar flux is equal to 1.136 times the value at Earth's orbit.

$1.136S_0$—the value required to achieve flux balance with the outgoing infrared radiation at the top of the atmosphere. Infrared fluxes have in this case been calculated at all levels; this extravagance is not retained in the calculations presented in the next section.

Figure 2 demonstrates that water vapor is a much better absorber of thermal infrared radiation than of visible and near-infrared radiation: The net infrared flux declines by a factor of nearly 1000 toward the surface, whereas the net solar flux decreases by only a factor of 3. The lower portion of this atmosphere should therefore be convective, as indeed it has been assumed to be. This prediction is in apparent conflict with the results of Watson et al. (1984), who found that the moist convective region of a water-rich atmosphere should be underlain by a region in radiative equilibrium. Their calculation is not strictly comparable to the one shown here; nevertheless, it is hard to reconcile their results with the large differences in visible and infrared opacities calculated by the present model. The most likely explanation for the difference between the two models is that their estimated opacities were lower, as indicated by
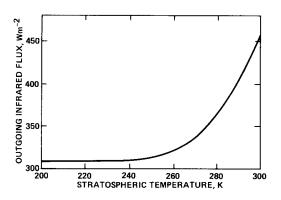
FIG. 3. Outgoing infrared flux (F_{IR}) at the top of a dense, moist greenhouse atmosphere as a function of the assumed stratospheric temperature. The surface temperature is 640°K.

the persistence of transmission windows near 1.02, 1.22, and 1.6 μm in the lower portion of their model atmosphere.

A related issue concerns my assumption that the lapse rate would follow a dry adiabat in the unsaturated region (Fig. 1b). It is not obvious that it should do so; Matsui and Abe (1986a,b), for example, calculated that the lapse rate here would be determined by radiative equilibrium. Their radiative model, however, was too crude to make this a reliable prediction. Watson et al. (1984) found that the lapse rate in the deep atmosphere was generally adiabatic, but was sometimes subadiabatic near the ground. This prediction is likewise suspect because of uncertainties in the infrared opacity of water vapor at high temperatures (see Section 2a). If the deep portions of a runaway greenhouse atmosphere are indeed stable, the surface temperatures calculated here will be somewhat too high. This, again, is in line with my goal of calculating upper limits on T_s.

The results are also rather insensitive to the assumed stratospheric temperature profile. To demonstrate this, I have plotted in Fig. 3 the outgoing infrared flux at the top of a dense, moist greenhouse atmosphere (T_s = 640°K) as a function of the stratospheric temperature T_o. (The stratosphere is assumed to be isothermal.) The figure

shows that F_{IR} is virtually independent of T_o provided that T_o is less than about 250°K. The reason is that the stratosphere is so tenuous at these high surface temperatures that its effect on the outgoing flux is negligible. This should be true for any atmosphere in which the stratosphere is water-dominated. For stratospheric temperatures greater than 250°K this would not be the case. However, with no ozone to heat it, such a warm stratosphere would not be expected for any planet outside the orbit of Venus.

3. RESULTS

(a) Response of Earth's Atmosphere to Increased Solar Flux

As an initial application, a series of model experiments was performed in which the surface temperature T_s was raised in a stepwise manner from 200 to 1800°K. The corresponding change in the H_2O vapor pressure at the surface is shown in Fig. 4. For T_s < 647.1°K, the critical point for water, the H_2O pressure follows the saturation vapor pressure curve. The atmosphere in this temperature regime is in the moist greenhouse state. A discontinuity occurs at the critical point because the remainder of the ocean would evaporate above this temperature. Above the critical point the H_2O
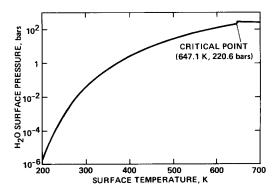

FIG. 4. Calculated vapor pressure of water at the Earth's surface as a function of surface temperature. Below the critical point this curve is just the saturation vapor pressure curve for water. Above the critical point the pressure is equivalent to that of a full terrestrial ocean.
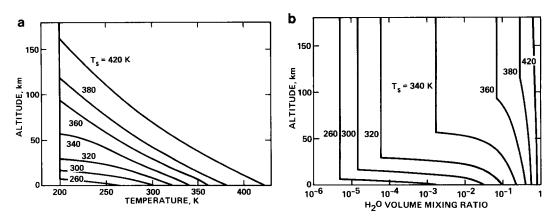
FIG. 5. Temperature (a) and H_2O volume mixing ratio (b) versus altitude for selected moist greenhouse atmospheres. The lower portions of the curves represent moist pseudoadiabats.

pressure is constant and the atmosphere is in the runaway greenhouse state. The total H_2O inventory assumed here is equal to the amount of water in Earth's oceans, 1.4×10^{24} g. When fully vaporized this produces a surface H_2O pressure of 270 bar—about 50 bar greater than the vapor pressure at the critical point. If the mass of the oceans was somewhat lower, the H_2O pressure at the surface would vary smoothly from the saturated to the unsaturated region, and the
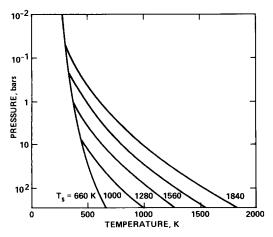

FIG. 6. Temperature versus pressure for selected runaway greenhouse atmospheres. The lower portions of the curves represent dry adiabats. The curve(s) to which they are all joined are moist pseudoadiabats, which are very nearly equivalent to the saturation vapor pressure curve for water.

transition from a moist to a runaway greenhouse would occur at a lower temperature.

Accompanying the increase in the H_2O vapor pressure at the surface is an increase in the depth of the convective region and an increase in the water content of the stratosphere. These changes are illustrated in Fig. 5. Because the surface pressure is variable, the profiles are most easily compared on an altitude scale. These results are similar to those shown in Figs. 3 and 4 of KPA. For a 1-bar background atmosphere the biggest change in stratospheric water vapor occurs at surface temperatures between 320 and 360°K, as the H_2O volume mixing ratio at the surface increases from about 0.1 to 0.4.

At surface temperatures above 647°K the atmosphere is in the runaway greenhouse state. Selected temperature profiles in this regime are shown in Fig. 6. The different curves represent dry adiabats in the lower atmosphere intersecting moist adiabats at various heights above the surface. At these surface temperatures the model atmosphere is composed of nearly 100% water vapor, so the moist adiabats are all close to the saturation vapor pressure curve. The curves are not actually identical because the water vapor mixing ratio is slightly different in each case.
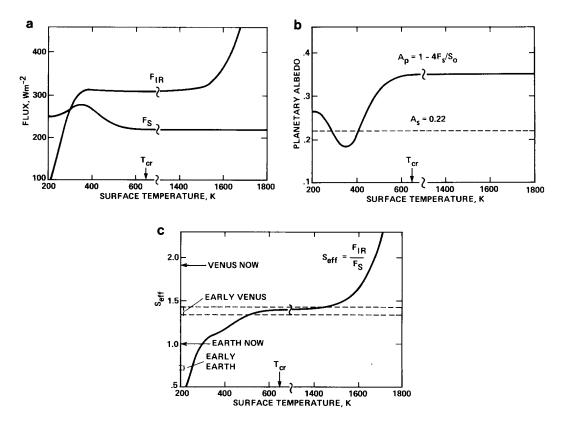
The radiative fluxes calculated for these

FIG. 7. Radiation fluxes and their derived functions versus temperature at the Earth's surface: (a) Net outgoing infrared flux F_{IR} and net incident solar flux F_S. (b) Planetary albedo A_p and surface albedo A_s. (c) Effective solar constant S_{eff}. The horizontal dashed lines in (c) represent estimates of the solar flux at Venus orbit 4.6 billion years ago. There is a break in the horizontal scale between 700 and 1300°K.

atmospheres are shown in Fig. 7. Figure 7a shows the net solar radiation flux F_S and the net infrared radiation flux F_{IR} as functions of surface temperature. Both fluxes are evaluated at the top of the model atmosphere. The solar constant in this calculation is assumed to be that for present Earth ($S_0 = 1360$ W m^{-2}). F_{IR} increases steeply as T_s is raised from 200 to 360°K, then levels out at higher surface temperatures at a value of about 310 W m^{-2}. For comparison, the predicted value of F_{IR} for the present (unsaturated) atmosphere is 268 W m^{-2}, according to this model. The reason that F_{IR} flattens out in this manner is that, as the moist convective layer thickens, the atmosphere becomes opaque to infrared radiation at all wavelengths. Only that part of the

atmosphere at pressure less than a few tenths of a bar is able to radiate to space; hence, continued deepening of the moist convective region has no effect on the outgoing infrared flux.

Above about 1400°K, F_{IR} once again begins to increase with T_s. The reason is that, at these extremely hot temperatures, the lower atmosphere and surface begin to radiate efficiently in the visible and near infrared, where the water vapor opacity is low. Detailed examination shows that almost all of the increase in F_{IR} between 1400 and 1700°K occurs at wavelengths shorter than 0.78 μm. At still higher surface temperatures the moist convective layer becomes thin enough that the lower atmosphere can radiate through it at longer wavelengths.

The net solar flux F_S increases at first as T_s is increased from 200 to 360°K, then decreases to a constant value ($\sim$220 W m^{-2}) at higher surface temperatures (Fig. 7a). The initial rise in F_S is caused by increased absorption of solar radiation by atmospheric H_2O. The subsequent decline at higher surface temperatures is caused by Rayleigh scattering. These changes are exhibited more clearly if one recasts F_S in terms of planetary albedo A_p ($= 1 - 4F_S/S_o$) (Fig. 7b). A_p goes through a minimum near $T_s = 360$°K, then approaches a constant value of 0.35 at temperatures above about 600°K. F_S and A_p continue to change long after F_{IR} has become constant because the atmosphere is much more transparent in the visible than in the infrared. A note of caution should, however, be interjected: The absorption coefficients used in the calculation of solar energy deposition were derived for a single temperature (300°K) only. Thus, the prediction that A_p becomes constant at high surface temperatures may not be reliable.

Having evaluated the dependence of the net solar and infrared fluxes upon surface temperature, one is now in a position to calculate T_s as a function of the solar constant. The net solar fluxes shown in Fig. 7a were computed under the assumption that the incident solar flux was equal to the present value at Earth's orbit (S_o). The value of F_S is, in general, different than that of F_{IR}. For an atmosphere in steady state, however, the net outgoing radiation must equal the net incident radiation. Thus, the effective value of the solar constant (normalized to S_o) required to support a given surface temperature must be given by $S_{eff} = F_{IR}/F_S$.

S_{eff} is plotted against T_s in Fig. 7c. According to this model the critical solar flux at which the greenhouse effect "runs away" is 1.4S_o. This is a particularly interesting result for the following reason: The solar flux at Venus' orbit is 1.91 times higher than the flux incident upon Earth. But the Sun has been getting brighter with time; shortly after being formed it was less

luminous than today by about 25 to 30% (Newman and Rood 1977, Gough 1981). The solar flux at Venus' orbit early in that planet's history should therefore have been between 1.34S_o and 1.43S_o. These limits are represented by the dashed lines in Fig. 7c. Since these limits neatly bracket the solar flux required for runaway, it is impossible to determine from the present calculation whether a cloud-free early Venus would have been in the moist or runaway greenhouse state. According to this model, the surface temperature could equally well have been 500 or 1500°K.

(b) Effect of Clouds

As mentioned earlier, clouds could have a strong influence on the radiation budget in a warm moist atmosphere. Since it is not known how cloudiness or cloud properties would vary with surface temperature, it does not seem particularly useful to repeat the calculations shown in Fig. 7 for different, ad hoc cloud models. It is instructive, however, to illustrate the effect of clouds on the model for a specific case. In particular, it is interesting to estimate how the transition from a moist to a runaway greenhouse would be affected by a cloud layer at various pressure levels. The model atmosphere chosen for this calculation has a surface temperature of 640°K, just below the critical point, and a surface pressure of some 203 bar. Cloud properties were determined by the criteria described in Section 2c. Cloud locations and optical depths are listed in Table I. For this calculation, the surface albedo was lowered from 0.22 to 0.05—a value appropriate for a water-covered surface. Changing the surface albedo has little effect by itself on the radiation budget because very little solar energy actually escapes from the surface.

Two sets of curves are shown in Fig. 8: the solid curves are for 100% cloud cover, and the dashed curves are for 50% cloud cover. In a real atmosphere, fractional cloudiness might be 50% or less at any given level, yet the net effect might be

TABLE I

CLOUD LEVELS AND CLOUD PROPERTIES

Pressure[a] (bar)	Altitude[a] (km)	Temperature[a] (°K)	Liquid water content (g m^{-3})	Optical depth at 0.55 μm
1.7(−5)	257	216	6.8(−6)	6.0(−3)
3.8(−4)	225	243	1.4(−4)	0.13
2.7(−3)	202	263	9.1(−4)	0.90
1.8(−2)	179	288	5.4(−3)	5.7
0.10	155	318	2.8(−2)	32
1.2	116	377	0.28	350
11	73	457	2.3	3000
151	8.9	615	39	3.7(4)

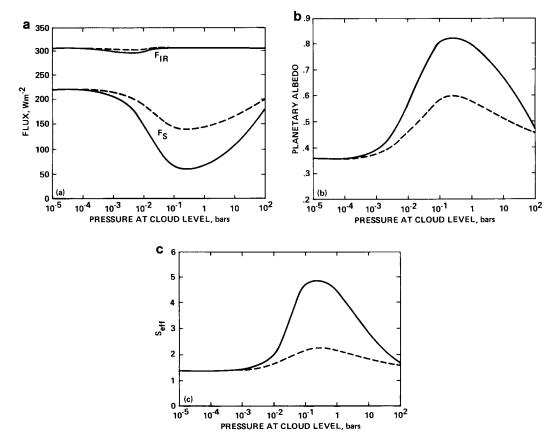[a] Values are listed at the midpoint of the cloud layer. Read 1.0(5) as 1.0 × 10^5.

FIG. 8. Effect of a single cloud layer on the radiation budget for a moist greenhouse atmosphere with a surface temperature of 640°K: (a) Net infrared flux F_{IR} and net solar flux F_S. (b) Planetary albedo. (c) Effective solar constant. Solid and dashed curves are for 100 and 50% cloud cover, respectively. The abscissa represents the pressure at the center of the cloud layer. Cloud properties are listed in Table I.

closer to complete coverage because clouds could be present at a variety of different levels. So it is not easy to predict which set of curves might be closer to the truth.

The effect of such a cloud on the net solar and infrared radiation fluxes is shown in Fig. 8a. F_{IR} is little affected by the cloud, regardless of where the cloud is located. The maximum decrease in F_{IR} is roughly 4% for a cloud level of a few millibars. Above this height, the cloud is so optically thin that it has little effect on the outgoing radiation; below this height, the atmosphere above the cloud becomes optically thick, so the effect of the cloud again disappears. F_S, on the other hand, is very strongly affected. For a cloud level of a few tenths of a bar, the net incident radiation is reduced by a factor of 3 or more. Equivalently, the planetary albedo increases from ~0.36 to as much as 0.8 (Fig. 8b). The effect of the cloud is much larger for solar radiation than it is for infrared, because the atmosphere is more transparent in the visible. Such an H_2O-rich atmosphere is fundamentally different from the present terrestrial atmosphere because of its greater infrared opacity. On the present Earth, the increase in albedo caused by clouds is partly compensated by their contribution to the greenhouse effect; hence, clouds can warm or cool the surface depending on their altitude and optical depth. By contrast, the effect of clouds in a warm, moist atmosphere should be a clearcut cooling of the planetary surface.

The critical solar flux at which a runaway greenhouse would occur is highly dependent on the presence of clouds (Fig. 8c). The cloud-free value, as just mentioned, is $1.4S_o$. For a cloud located at a few tenths of a bar pressure, the critical flux increases to $2.2S_o$ for 50% cloud cover, or to $4.8S_o$ for 100% cloud cover. These results imply that liquid water might well exist on the surface of Venus even today if the total water inventory was comparable to that of Earth. Early Venus was therefore quite likely to have been cool enough to maintain oceans.
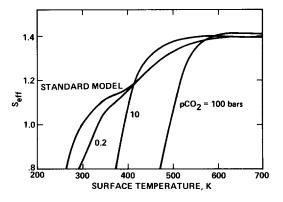

FIG. 9. Effective solar constant S_{eff} required to maintain a given surface temperature at selected CO_2 pressures.

(c) Other Sensitivity Studies and Comparisons with Previous Models

The results presented thus far were for an assumed CO_2 mixing ratio of 3×10^{-4}, similar to modern Earth. An obvious question is how sensitive the results are to the concentration of CO_2. The answer to this question is presented in Fig. 9. Here, S_{eff} is plotted against surface temperature for CO_2 pressures ranging up to 100 bar. At low values of S_{eff}, T_s increases monotonically with increasing pCO_2. However, CO_2 increases alone are not able to trigger a runaway greenhouse. This behavior is in accord with the predictions of Kasting and Ackerman (1986), who studied the response of surface temperature to increased CO_2 levels for S_{eff} equal to 0.7 and 1.0. At values of S_{eff} between 1.2 and 1.35 something unusual occurs: T_s decreases as pCO_2 increases from 0.2 to 10 bar, then increases once again at $pCO_2 = 100$ bar. The reason is that, at $pCO_2 = 10$ bar, the increase in total surface pressure outstrips the increase in saturation vapor pressure caused by the greenhouse effect; hence, the surface water vapor mixing ratio declines and the stratosphere dries out. A similar but less pronounced effect is predicted for $S_{eff} = 1$ (Kasting and Ackerman 1986).

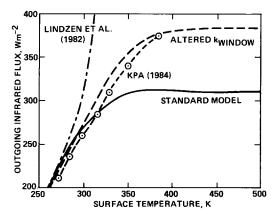The key point illustrated by Fig. 9, however, is that increases in CO_2 have little ef-

FIG. 10. Outgoing infrared flux F_{IR} versus surface temperature for different models. The curve labeled "altered k_{window}" shows the effect of using Matsui and Abe's H_2O absorption coefficient in the 8- to 12-μm window region.

fect on the solar flux required to trigger a runaway greenhouse. For $pCO_2 \leq 10$ bar, the critical value of S_{eff} remains equal to 1.4; for $pCO_2 = 100$ bar, it increases to 1.42. The reason that the effect of CO_2 is small in this model is that Earth's oceans contain 270 bar of water—enough to dilute anything else in the atmosphere. If pCO_2 was greater than 100 bar, or if the ocean was smaller, the influence of CO_2 would be more apparent.

Another parameter of obvious importance is the H_2O absorption coefficient in the 8- to 12-μm window region. The formulation employed here, from Roberts et al. (1976), presumes an exponential dependence on temperature and a quadratic dependence on pH_2O. By contrast, the gray atmosphere model of Matsui and Abe (1986a,b) assumes an H_2O absorption coefficient of 0.1 cm^2 g^{-1} bar^{-1}, supposedly valid within the window region. To compare with their results I performed a set of model experiments using their absorption coefficient between 8 and 12 μm. The effect on the outgoing infrared flux is shown by the curve labeled "altered k_{window}" in Fig. 10. F_{IR} in the transition region (400 to 1400°C) increases from 310 to 383 W m^{-2}. Matsui and Abe's model atmosphere is obviously more

transparent to infrared radiation than even the least opaque spectral region in the present model.

Also shown in Fig. 10 are calculations of F_{IR} versus T_s from the models of Lindzen et al. (1982) and KPA. KPA's curve fails to flatten out at high surface temperatures because their model did not include all the weak H_2O bands in the near infrared (Section 2a). The model of Lindzen et al. predicts exactly the inverse type of asymptotic behavior from that found here: their curve goes off the graph vertically instead of horizontally. As discussed in Section 1, this behavior is nonphysical because it requires that the planet radiate energy with more than the maximum possible efficiency.

A second parameter of interest is the H_2O absorption coefficient in the visible and near infrared. In addition to becoming important to the thermal radiation budget at high surface temperatures, absorption in this spectral region strongly affects the planetary albedo. The present model parameterizes H_2O absorption in this spectral region using standard, rotation–vibration band models (Appendix B), which are then fitted to exponential sums for use in the scattering calculation. By contrast, Vardavas and Carver (1985) assumed that H_2O absorbs in a continuum down to either 0.55 or 0.45 μm, depending on whether one believes their text or Table 6 of Vardavas and Carver (1984). This assumption was based on atmospheric measurements made by Tomasi (1979a,b). The strong absorption which they calculate causes their planetary albedo to decrease strongly at high H_2O levels and could explain why their model "runs away" for a mere 2% increase in the solar constant.

To determine the effect on my model, I performed a set of calculations using Tomasi's absorption coefficients between 0.55 and 1 μm. The change in planetary albedo is shown by the dashed curve in Fig. 11. A_p decreases more dramatically near $T_s = 350°K$ than in my model and recovers to a lower value at high T_s. The net result is to
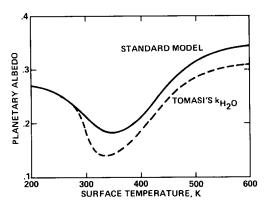
FIG. 11. Planetary albedo A_p versus surface temperature for the standard model and for a model in which Tomasi's continuum H_2O absorption coefficients are used in the visible and near infrared.

lower the critical solar flux for runaway from $1.4S_0$ to $1.33S_0$ (Fig. 12). This does not explain why Vardavas and Carver's model predicts runaway at only $1.02S_0$ for the same, fully saturated conditions. Their results are also shown in Fig. 12. The range of T_s that they have covered is relatively small; it may be that they would have reached a different conclusion had they extended their calculations to higher surface temperatures.

(d) Runaway Greenhouses during Accretion

Impact devolatilization of incoming planetesimals should have released H_2O and CO_2 directly into the atmosphere during the Earth's accretion. Matsui and Abe (1986a) have studied the effect of a pure H_2O protoatmosphere on the Earth's early thermal evolution using a simple analytic radiation model. They predicted that the growing Earth would have had a 100-bar steam atmosphere with a surface temperature near 1500°K—above the solidus for typical silicate rocks. Other thermal evolution models (e.g., Coradini et al. 1983) which ignore the blanketing effect of the atmosphere predict a thin, solid crust and a surface temperature near 300°K.

Matsui and Abe's atmospheric model

was gray and radiatively equilibrated at all heights. They considered the possibility of (dry) convection, but dismissed it because their calculated radiative lapse rate was subadiabatic—probably because their assumed H_2O opacity was smaller than the actual opacity throughout much of the infrared (see previous section).

The present model is ideally suited for checking their calculation. The existence of a substantial accretionary heat flux at the surface would require that the atmosphere was almost certainly convective throughout its lowermost regions, Matsui and Abe's result notwithstanding. This may be seen from inspection of Fig. 2. If the accretionary heat flux was some appreciable fraction of the solar constant, it would be much larger than the energy flux that could be transmitted radiatively through the lower atmosphere. Hence, the thermal structure assumed here should be appropriate. If the solar flux incident at the top of the atmosphere is assumed to be constant, the difference between the net incoming solar flux and the net outgoing infrared flux can be reinterpreted as the accretionary heat flux required to sustain a given surface temperature. Assuming that the solar luminosity was 30% less than today at the time when
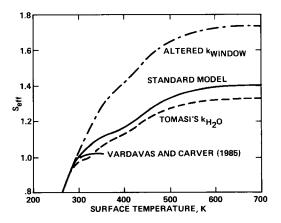

FIG. 12. Effective solar constant S_{eff} versus surface temperature for different models. The dashed curves correspond to the models discussed in the captions to Figs. 9 and 10.
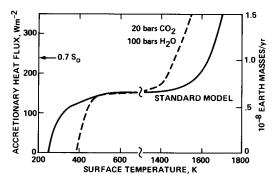
FIG. 13. Accretionary heat flux required to maintain a given surface temperature on the evolving Earth. The right-hand scale shows the equivalent mass accretion rate for the fully formed planet. The solar constant is assumed to be $0.7S_o$.

Earth was forming, the accretionary heat flux is given by $F_{acc} = F_{IR} - 0.7F_S$. This interpretation is, of course, meaningful only if F_{acc} is positive.

The solid curve in Fig. 13 shows the result of recasting the radiation fluxes from the standard model (Fig. 7a) in this manner. The critical value of F_{acc} required to trigger runaway greenhouse conditions is about 150 W m^{-2}, or 63% of the globally averaged solar flux at the time that the Earth was forming. For an Earth-sized object, this corresponds to an accretion rate of 0.64 × 10^{-8} Earth masses (M_o) year^{-1}. This may be compared with an estimated accretion rate of about 1 × 10$^{-8}M_o$ year^{-1} at the time when Earth was about 90% formed (Safronov 1972, Matsui and Abe 1986a). The actual accretion rate is highly uncertain; it could vary up or down by as much as an order of magnitude. For the values assumed by Matsui and Abe, however, it appears that their conclusion is fundamentally correct: The surface heat flux on a growing Earth would have been sufficient to vaporize any water that was present, creating a dense steam atmosphere.

A more meaningful comparison can be obtained by assuming that the protosphere contained 100 bar of water, as in Matsui and Abe's model, in place of the 270 bar assumed in my standard model. To this I have added 20 bar of CO_2, based on the estimate by Holland (1984, Chapter 2) that one-third of Earth's carbon dioxide was in the atmosphere at the close of accretion. The result is shown by the dashed line in Fig. 13. This atmosphere is hotter than the standard model at low values of F_{acc} because of the warming provided by CO_2. Conversely, it is cooler at high values of F_{acc} because the dry convective region is shallower. The surface temperature predicted for a mass accretion rate of 10$^{-8}M_o$ year^{-1} is about 1500°K, in good agreement with Matsui and Abe (1986a). The fact that the two models agree this well is to some extent fortuitous; nonetheless, it implies that the calculation is reasonably robust.

Clouds would of course affect these results as well, although their influence would be smaller than in the pure solar heating case because a substantial fraction of the heat input is from below. Figure 8a shows that the effect of clouds on the outgoing infrared radiation would have been small, regardless of where the heat was coming from. Thus, their main effect would have been to reflect some portion of the incident solar radiation. If all of the incident radiation was reflected, the critical value of F_{acc} required for runaway would increase by about a factor of 2. This might shorten the duration of a steam atmosphere on the accreting Earth, but it does not alter the prediction that such an atmosphere could once have existed. Accretionary atmospheres have been examined in more detail by Zahnle et al. (1987).

4. DISCUSSION

The results presented in the last section provide a basis for understanding how the atmosphere of Venus may have evolved. The cloud-free calculations (Fig. 7) put early Venus right on the borderline between a moist and a runaway greenhouse. Since clouds should have tended to cool the surface (Section 3b), early Venus would almost certainly have been in the moist greenhouse state, provided that its initial

endowment of water was similar to that of Earth. This was also the conclusion reached by KPA. They favored this hypothesis for several reasons in addition to their surface temperature calculations: First, they argued that it provides a more satisfactory explanation for the presently observed D/H ratio in the Venus clouds in that it does not require prolonged outgassing of isotopically light, juvenile water to prevent the atmospheric D/H ratio from becoming even higher than observed. Second, it shortens the time required for water loss by providing a mechanism (carbonate formation) for sequestering CO_2, thereby keeping the background atmosphere relatively thin. And, third, the oxygen left behind by the escape of hydrogen could have been more easily removed by weathering in the presence of liquid water.

Of these three points, only the second now appears to be a valid concern. If the surface temperature of a runaway greenhouse atmosphere is indeed above the melting point of the crust, as found both here and in the calculations by Watson et al. (1984) and Matsui and Abe (1986a,b), oxygen could have been lost very rapidly by reaction with the magma. Oxygen could also have been dragged out to space along with the escaping hydrogen if the solar EUV flux powering this process were enhanced at that time (Zahnle and Kasting 1986). Thus, getting rid of the oxygen seems not to be a problem for either the moist or the runaway greenhouse model. At the same time, the D/H enrichment in the Venus clouds now seems to be telling us less than was once thought. The traditional interpretation (Donahue et al. 1982) is that the factor of 100 enrichment in D/H requires that Venus started out with at least 100 times as much water as it has now, or more if some deuterium escaped along with the hydrogen. But this is true only if there has been no substantial influx of water into Venus' atmosphere. Recently, Grinspoon and Lewis (1988) have argued (convincingly) that Venus' water is in steady state:

the loss of hydrogen to space is balanced by a continued input of water from comets or from delayed juvenile outgassing. If this is true, then no increase in Venus' past water inventory is required to explain the observed D/H ratio. The enrichment could result simply from preferential escape of the lighter isotope during the recent past (Hunten et al. 1988). Hence, Venus could conceivably have started out dry, as originally suggested by Lewis (1972), in which case the whole question of moist versus runaway greenhouse atmospheres would become somewhat moot.

A wet origin for Venus is still favored if one accepts the argument that mixing between the accretion zones of Venus and Earth, as predicted by the model of Wetherill (1985), would have resulted in comparable initial volatile inventories for the two planets. Thus, the question of how Venus could have lost its water is still relevant, even if the isotopic evidence for this event is no longer accepted. The key issue concerning water loss is not whether Venus' atmosphere was in a moist or a runaway greenhouse state, but rather, the rate at which water could have been lost through photodissociation followed by hydrogen escape. This rate is proportional to the mixing ratio of water vapor in the stratosphere $f_o(H_2O)$ (Hunten 1973), which is in turn related to the H_2O mixing ratio near the surface (Ingersoll 1969). The results shown in Figs. 5a and 7c can be combined to yield $f_o(H_2O)$ as a function of the solar constant (Fig. 14). For a fully saturated, cloud-free model, the water vapor content of the stratosphere increases dramatically for solar fluxes greater than about $1.1S_o$. Any value of $f_o(H_2O)$ in excess of 10^{-3} may be considered unstable because it would lead to the escape of Earth's oceans in less than about 4 billion years, if hydrogen escaped at the diffusion limit. Since a 10% increase in solar flux corresponds to moving the Earth 5% closer to the Sun, these results are in agreement with those of Hart (1978), who concluded (for different rea-
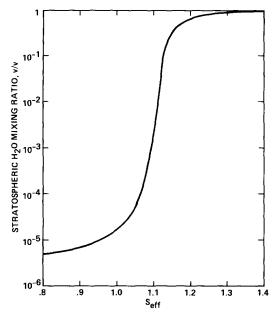
FIG. 14. H_2O volume mixing ratio in the stratosphere versus effective solar constant S_{eff}.

sons) that the inner edge of the continuously habitable zone (CHZ) was near 0.95 AU. The actual boundary of the CHZ should in reality lie somewhat closer to the Sun, because the assumptions made here concerning clouds and relative humidity should tend to overestimate both the surface temperature and the rate of water loss at a given solar flux. The solar constant is currently increasing at a rate of a little under 1% per hundred million years (Gough 1981). Thus, the present model suggests that Earth could begin to lose its oceans around one billion years hence. The actual time remaining before this process begins is probably longer than this, because the model yields upper limits on surface temperature and because further decreases in atmospheric pCO_2 brought about by the carbonate–silicate cycle could slow the predicted climatic warming (Walker et al. 1981). Thus, the loss of Earth's water is not something that we will have to worry about for a very long time.

5. CONCLUSION

Calculations with a fully saturated, cloud-free, climate model indicate that the critical solar flux required to trigger a runaway greenhouse is 1.4 times the values at Earth's orbit, or about the same as the flux at Venus' orbit early in Solar System history. This result is nearly independent of the amount of CO_2 in the atmosphere, but is sensitive to the H_2O absorption coefficient in the 8- to 12-μm window region. The presence of even a single-layer cloud could have increased the critical solar flux to between $2S_0$ and $5S_0$. Thus, if Venus started out with an Earth-like water endowment, it ought once to have had oceans upon its surface.

A runaway greenhouse atmosphere was probably present on Earth throughout much of the process of accretion. The surface temperature of a 100-bar steam atmosphere should have been about 1500°K, in agreement with previous predictions. This finding provides additional support for the idea that the Earth's surface was molten at this time.

Earth's atmosphere is apparently stable with respect to water loss for solar flux increases of less than 10%. Still larger solar flux increases could cause the stratosphere to become wet, resulting in rapid loss of water from photodissociation followed by hydrogen escape. The Earth might therefore be uninhabitable had it formed approximately 5% closer to the Sun. Earth may lose its oceans and revert to its original lifeless state beginning about one billion years hence.

APPENDIX A: ADIABATIC LAPSE RATES IN NONIDEAL ATMOSPHERES

The rate at which temperature decreases during the adiabatic expansion of a mixture of a nonideal, condensable gas (water vapor) and an ideal, noncondensable gas (CO_2 or N_2) was calculated in the following manner. The total pressure P was assumed to be given by

$$P = P_v + P_n, \qquad (A1)$$

$$P_v = \rho_v RT/(\beta m_v). \qquad (A2)$$

where P_v is the vapor pressure of water and P_n is the pressure exerted by the noncondensable gas. P_n is related to the density ρ_n of the noncondensable gas by the perfect gas law: $P_n = \rho_n RT/m_n$, where R is the universal gas constant, T is temperature, and m_n is the gram molecular weight of the gas. P_v and ρ_v are related in a more complicated manner. I have calculated their relationship, as well as the values of other thermodynamic quantities, using the computer program listed in Appendix B of the *NBS/NRC Steam Tables* (Haar et al. 1984). The results of the program were expressed in the form

Here, $\beta = \beta(\rho_v, T)$ is a parameter that expresses the degree to which the gas departs from ideality. The value of β for water vapor ranges from near unity at low pressures and high temperatures to above 4 near the critical point. Following Ingersoll (1969), I also define the ratio

$$\alpha_v = \rho_v/\rho_n. \qquad (A3)$$

This parameter is constant except where condensation is occurring.

The variation of α_v with temperature in the condensation region is given by Eq. (A7) in Ingersoll (1969), which I rewrite as

$$\frac{d \ln \alpha_v}{d \ln T} = \frac{(R/m_n)(d \ln \rho_v/d \ln T) - C_{vn} - \alpha_v(d\, s_v/d \ln T) - \alpha_c(d\, s_c/d \ln T)}{\alpha_v(s_v - s_c) + R/m_n}. \qquad (A4)$$

Here, C_{vn} is the specific heat (per gram) at constant volume of the noncondensable gas, s_v is the specific entropy (per gram) of the vapor, and α_c and s_c are the density ratio (ρ_c/ρ_n) and specific entropy of the condensed phase (water or ice). I assume that a gas parcel in the atmosphere would follow a pseudoadiabatic expansion, in which the condensed phase leaves the system immediately ($\alpha_c = 0$).

The variation of pressure with temperature in the condensation region, i.e., the inverse of the moist adiabatic lapse rate, may be obtained by differentiating Eq. (A1), making use of (A3) and the perfect gas law. The result is

$$\frac{d \ln P}{d \ln T} = \frac{P_v}{P} \frac{d \ln P_v}{d \ln T}$$
$$+ \frac{P_n}{P}\left[1 + \frac{d \ln \rho_v}{d \ln T} - \frac{d \ln \alpha_v}{d \ln T}\right]. \qquad (A5)$$

The derivatives of P_v and ρ_v with respect to temperature were evaluated by taking the difference of successive values calculated at 5 degree intervals along the saturation vapor pressure curve.

Equations (A4) and (A5) have simpler analogs in the temperature regime (below $\sim100°C$) where water vapor behaves like an ideal gas and where the Clausius–Clapeyron equation

$$\frac{d \ln P_v}{d \ln T} = \frac{m_v L}{RT} \qquad (A6)$$

is valid. Here L is the latent heat (per gram) of evaporation or sublimation. These equations are repeated here because they have been expressed incorrectly in two other papers (Kasting et al. 1984a, Vardavas and Carver 1985). The correct results are

$$\frac{d\, \alpha_v}{d \ln T} = \left(\frac{m_v L}{m_n T} - \gamma\right)\Big/\left(\frac{L}{T} + \frac{R}{\alpha_v m_n}\right)$$

$$\gamma = C_{pn} + \alpha_c C_c$$

$$+ \alpha_v \left(C_c - \frac{L}{T} + \frac{dL}{dT}\right) \qquad (A7)$$

and

$$\frac{d \ln P}{d \ln T} = \frac{m_v L}{RT}$$

$$- \frac{1}{1 + \alpha_v m_n/m_v} \frac{d \ln \alpha_v}{d \ln T}. \qquad (A8)$$

The quantities C_{pn} and C_c are, respectively, the specific heats (per gram) at constant pressure for the noncondensable gas and the condensed phase. The value of dL/dT may be assumed to be equal to zero below 0°C; above this temperature its value (from Kirchoff's equation) is

$$\frac{dL}{dT} = c_{pv} - c_w$$
$$\equiv -A \simeq -0.553 \text{ cal g}^{-1} \text{ °K.} \quad \text{(A9)}$$

Equations (A7) and (A8) are used in the present model only at temperatures below 0°C. With (A9), however, they are accurate to within a few percent up to at least 100°C. The saturation vapor pressure in this range can be obtained by integrating Eq. (A6) to obtain Magnus' equation (Iribarne and Godsen 1981, Eq. (4-53)):

$$p_v = p_0(T_0/T)^{m_v A/R}$$
$$\exp\left[\frac{m_v(L_0 + AT_0)}{R}\left(\frac{1}{T_0} - \frac{1}{T}\right)\right]. \quad \text{(A10)}$$

Equations (A7)–(A10) provide a convenient way of treating water in most model calculations.

The variation of pressure with temperature in the unsaturated region, i.e., the inverse of the dry adiabatic lapse rate, may be obtained by differentiating Eq. (A1), taking into account the fact that α_v is now constant. The (trivial) result is

$$\frac{d \ln P}{d \ln T} = \frac{P_v}{P}\left(\frac{\partial \ln P_v}{\partial \ln T}\right)_s$$
$$+ \frac{P_n}{P}\left(\frac{\partial \ln P_n}{\partial \ln T}\right)_s. \quad \text{(A11)}$$

The terms in parentheses represent partial derivatives at constant entropy. By using the second law of thermodynamics and a Maxwell's relation, one can show that for any fluid

$$\left(\frac{\partial \ln P}{\partial \ln T}\right)_s = \frac{C_p}{P(\partial V/\partial T)_P}, \quad \text{(A12)}$$

where V is the specific volume ($= 1/\rho$). For water vapor, the term $(\partial V/\partial T)_P$ was evaluated from the thermodynamic computer program. For the ideal gas, $P(\partial V/\partial T)_P = R/m_n$.

The behavior of water vapor in the immediate vicinity of the critical point is complicated. Ingersoll (1969) has pointed out that it may be incorrect to treat water vapor and the noncondensable gas separately, in which case Eqs. (A1), (A4), and (A5) are invalid. This is not a serious problem for most cases of physical interest because, in a real atmosphere, the pressure–temperature curve generally would not come near the critical point. This is because the surface temperature jumps abruptly from near 500°K to about 1500°K (Fig. 6c); thus, the critical temperature should usually be encountered within the undersaturated region. The calculations described here do approach the critical point, and the calculated lapse rates may be inaccurate in this region. To avoid generating any obviously unphysical results, I set the derivative $ds_v/d(\ln T)$ in Eq. (A4) equal to zero at the critical point. Then, since $\alpha_c = 0$ and since $(s_v - s_c)$ also goes to zero at this point, the moist lapse rate (Eq. (A5)) reduces to

$$\frac{d \ln P}{d \ln T} = \frac{P_v}{P}\frac{d \ln P_v}{d \ln T} + \frac{P_n}{P}\frac{C_{pn}m_n}{R}, \quad \text{(A13)}$$

which is the same as Eq. (A11) for the dry lapse rate except that the derivative of the vapor pressure is evaluated differently. For pure water vapor $d(\ln P)/d(\ln T)$ jumps from about 5.5 in the unsaturated region to 7.7 in the saturated region near the critical point, according to this model.

The lapse rate formulations given here were implemented in the radiative-convective model by using the computer program of Haar et al. (1984) to generate two tables. The first table contained values of β, P_v, $d(\ln P_v)/d(\ln T)$, $s_v - s_c$, $ds_v/d(\ln T)$, $ds_c/d(\ln T)$, and $d(\ln \rho)/d(\ln T)$ at 5 degree intervals along the saturation vapor pressure curve, from 0 to 374°C. The second table, which was used in the unsaturated region, contained values of β and $[\partial(\ln P_v)/\partial(\ln T)]_s$ for pressures of 1 to 345 bar and temperatures of 0 to 2000°C. ΔP for this table was 5

bar; ΔT was 10° below 600°C and 100° above that temperature. Values at specific (P, T) points in the unsaturated region were obtained by linear interpolation, taking care to use tabulated values on the proper (low-P, high-T) side of the saturation vapor pressure curve.

APPENDIX B: H_2O ABSORPTION IN THE VISIBLE AND NEAR-INFRARED

Absorption of solar radiation by water vapor plays an important role in determining the planetary albedo in a warm, moist atmosphere. This point was made clearly in the study by Vardavas and Carver (1985). Their albedo calculation, however, incorporates estimates by Tomasi (1979a,b) of H_2O continuum absorption in the visible and near-infrared parts of the spectrum. Tomasi reports a continuum mass absorption coefficient $\kappa(\lambda, 0°C)$ of 0.017 cm² g⁻¹ bar⁻¹ at 1.63 μm increasing to 0.03 cm² g⁻¹ bar⁻¹ at 0.55 μm. The continuum is presumed to arise from absorption in the far wings of rotation–vibration bands. Although Tomasi labels it "weak" absorption, this continuum, if it existed, would overwhelm Rayleigh scattering in a pure H_2O atmosphere by a factor of 200 at 0.55 μm.

The continuum measurements of Tomasi were derived from measurements of atmospheric attenuation along vertical and horizontal paths in various "window" regions in the visible and near-IR. There are two problems with Tomasi's analysis. First, most of the observed attenuation is a result of scattering by aerosols, and this component must be removed in order to calculate the absorption by water vapor. In principle this can be done, but in practice it is always difficult to calculate a small number from the difference between two larger ones. Evidence that Tomasi's procedure failed is provided by the fact that the measured continuum absorption coefficient increases at wavelengths below 1 μm, just as would be predicted for scattering by aerosols (Toon and Pollack 1976). If the absorption were
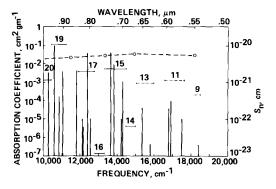

FIG. 15. Estimates of H_2O absorption in the visible and near infrared. The vertical lines represent band strengths S_n from Goody (1964). The horizontal bars represent the product xy_0 of the random band model parameters in various spectral intervals given in Table II. (Dashed bars are derived by extrapolation—see text.) The long dashed line indicates the water vapor continuum measured by Tomasi (1979b).

due solely to H_2O, by contrast, it ought to become weaker at shorter wavelengths.

A second, equally serious problem is that the "window" regions examined by Tomasi (1979a), at 0.665, 0.682, 0.715, 0.755, 0.784, 0.881, 1.01, 1.05, 1.09, 1.24, and 1.29 μm, all contain well-known rotation–vibration bands. Band intensities for the strongest of these, and for several (weaker) transitions in the visible, are shown in Fig. 15. It is likely that Tomasi did observe H_2O absorption at these wavelengths, but there is no obvious reason why it should be ascribed to a continuum. Line absorption by water vapor can be well described by the random band model suggested by Goody (1964). For Tomasi's conditions the band absorption may have been on the linear part of the curve of growth, giving a linear relationship between the observed extinction and water vapor abundances. But at the long pathlengths relevant to warmer conditions the optical depth in the Goody model increases as the square root of the absorber amount, rather than linearly as would be the case for a continuum.

In the present model I have calculated H_2O absorption in the visible and near-infrared by using the band model approach.

TABLE II

Selected Spectral Intervals and Random
Band Model Parameters at 1 bar and 300°K

Interval	Wavelength range (μm)	x	y_0
9	0.5400–0.5495	0.00141[a]	0.143[a]
10	0.5495–0.5666		
11	0.5666–0.6050	0.00912[a]	0.143[a]
12	0.6050–0.6250		
13	0.6250–0.6667	0.00646[a]	0.143[a]
14	0.6667–0.691	0.0014	0.0028
15	0.691 –0.752	0.038	0.143
16	0.752 –0.784	5.6(−5)	0.0025
17	0.784 –0.842	0.0339	0.107
18	0.842 –0.891		
19	0.891 –0.962	0.607	0.18
20	0.962 –1.036	0.620	0.0021

[a] These parameters derived by scaling relative to interval 15 (see text).

For water vapor bands longward of 0.67 μm, synthetic absorption coefficient spectra were computed as functions of temperature and pressure using the AFGL tape and line profile algorithms developed at AFGL (Smith et al. 1978, Clough and Kneizys 1979). These spectra were then used to compute transmission as a function pathlength, and the resulting transmission curves were fit to the Goody model

$$T = \exp\left[\frac{-xm}{(1 + xm/y)^{1/2}}\right] \qquad \text{(B1)}$$

to get the random band model parameters listed in Table II. In Eq. (B1) m is the absorber pathlength in g cm^{-2} and $y = y_0(P/P_0)$, where P is pressure and y_0 is the value of y at 1 bar.

For intervals shortward of 0.67 μm, where no information was available on the AFGL tape, a different procedure was used to estimate band model parameters. Three of these intervals (9, 11, and 13) contain well-known interference lines in the Fraunhoffer spectrum (Moore et al. 1966). The values of y_0 for these intervals were assumed to be the same as in interval 15.

The x's in these intervals were obtained by summing the equivalent widths of individual lines tabulated by Moore et al. and then scaling the value of x_{15} by the ratio of $(W/\Delta\nu)_i/(W/\Delta\nu)_{15}$. Here, W is the total equivalent width of absorption lines within an interval and $\Delta\nu$ is the total width of the interval. This approximate scaling follows from the observation that the transmission function for random spaced lines of equal intensity is given by $\exp(-W/\Delta\nu)$ and that the equivalent widths are on the linear part of the curve of growth for the observations of Moore et al.

In the long pathlength limit the Goody transmission function (Eq. (B1)) reduces to $T = \exp(-(xmy)^{1/2})$. Thus, for comparative purposes I have also plotted in Fig. 14 the product xy_0 in each interval, along with Tomasi's calculated continuum absorption coefficients. It is evident that the band model predicts decreasing absorption at short wavelengths, whereas the continuum model predicts just the opposite. The disparity between the two formulations is illustrated more directly by Fig.
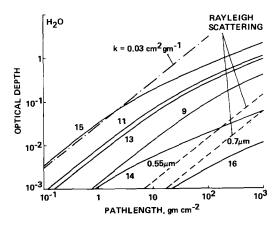

Fig. 16. Optical depth as a function of H$_2$O column abundance along horizontal path at 1 bar and 300°K. Solid curves represent random band models (see Fig. 15); the dash–dot line represents Tomasi's continuum at 0.55 μm; and the dashed lines indicate Rayleigh scattering by water vapor at two different wavelengths. For comparison, the Rayleigh optical depth of a dry, 1-bar, N$_2$–O$_2$ atmosphere is about 0.035 at 0.7 μm and 0.091 at 0.55 μm.

16, which shows optical depth at 1 bar as a function of absorber amount for the band models and for a continuum coefficient of 0.03 cm^2 g^{-1} (Tomasi's value at 0.55 μm). The band models predict substantially less absorption in every interval shortward of 0.78 μm, particularly at long pathlengths where the square root law is in effect. One should note that a pathlength of 10^3 g cm^{-2} corresponds to the vertical column depth of a 1-bar, pure H$_2$O atmosphere. Note also that the amount of absorption in most intervals significantly exceeds the attenuation by Rayleigh scattering for pure H$_2$O and should therefore become important for high water vapor abundances.

REFERENCES

BURCH, D. E., D. A. GRYVNAK, AND J. D. PEMBROKE 1971. *Investigation of the absorption of Infrared Radiation by Atmospheric Gases: Water, Nitrogen, and Nitrous Oxide*. AFCRL-71-0124, Bedford, MA.

CLOUGH, S. A., AND F. X. KNEIZYS 1979. Convolution algorithm for the Lorentz function. *Appl. Opt.* **18,** 2329.

CORADINI, A., C. FEDERICO, AND P. LANCIANO 1983. Earth and Mars: Early thermal profiles. *Phys. Earth Planet. Inter.* **31,** 145–160.

DONAHUE, T. M., J. H. HOFFMAN, R. R. HODGES, JR., AND A. J. WATSON 1982. Venus was wet: A measurement of the ratio of D to H. *Science* **216,** 630–633.

GOODY, R. M. 1964. *Atmospheric Radiation*. Oxford Univ. Press (Clarendon), London/New York.

GOUGH, D. O. 1981. Solar interior structure and luminosity variations. *Solar Phys.* **74,** 21–34.

GRINSPOON, D. H., AND J. S. LEWIS 1988. Comet impacts and the evolution of water and deuterium abundances on Venus. *Icarus*, in press.

HAAR, L., J. S. GALLAGHER, AND G. S. KELL 1984. *NBS/NRC Steam Tables*. Hemisphere Publishing Corporation, New York.

HART, M. H. 1978. The evolution of the atmosphere of the Earth. *Icarus* **33,** 23–39.

HERZBERG, G., AND L. HERZBERG 1953. Rotation-vibration spectra of diatomic and simple polyatomic molecules with long absorbing paths. XI. The spectrum of carbon dioxide (CO$_2$) below 1.25 μ. *J. Opt. Soc. Amer.* **43,** 1037–1044.

HOLLAND, H. D. 1984. *The Chemical Evolution of the Atmosphere and Oceans*. Princeton Univ. Press, Princeton, NJ.

HOWARD, J. N., D. L. BURCH, AND D. WILLIAMS 1956. Near-infrared transmission through synthetic atmospheres. *J. Opt. Soc. Amer.* **46,** 186–190.

HUNTEN, D. M. 1973. The escape of light gases from planetary atmospheres. *J. Atmos. Sci.* **30,** 1481–1494.

HUNTEN, D. M., T. M. DONAHUE, J. F. KASTING, AND J. C. G. WALKER 1988. Escape of atmospheres and loss of water. In *Origin and Evolution of Planetary and Satellite Atmospheres* (J. B. Pollack, S. K. Atreya, and M. S. Matthews, Eds.). Univ. of Arizona Press, Tucson, submitted for publication.

INGERSOLL, A. P. 1969. The runaway greenhouse: A history of water on Venus. *J. Atmos. Sci.* **26,** 1191–1198.

IRIBARNE, J. V., AND W. L. GODSEN 1981. *Atmospheric Thermodynamics*, 2nd ed. Reidel, Dordrecht.

KASTING, J. F., AND T. P. ACKERMAN 1986. Climatic consequences of very high CO$_2$ levels in Earth's early atmosphere. *Science* **234,** 1383–1385.

KASTING, J. F., J. B. POLLACK, AND T. P. ACKERMAN 1984. Response of Earth's atmosphere to increases in solar flux and implications for loss of water from Venus. *Icarus* **57,** 335–355.

LAL, M., AND V. RAMANATHAN 1984. The effects of moist convection and water vapor radiative processes on climate sensitivity. *J. Atmos. Sci.* **41,** 2238–2249.

LEWIS, J. S. 1972. Low temperature condensation from the solar nebula. *Icarus* **16,** 241–252.

LINDZEN, R. S., A. Y. HOU, AND B. F. FARRELL 1982. The role of convective model choice in calculating the climatic impact of doubling CO$_2$. *J. Atmos. Sci.* **39,** 1189–1205.

MANABE, S., AND R. T. WETHERALD 1967. Thermal equilibrium of the atmosphere with a given distribution of relative humidity. *J. Atmos. Sci.* **24,** 241–259.

MATSUI, T., AND Y. ABE 1986a. Evolution of an impact-induced atmosphere and magma ocean on the accreting Earth. *Nature* **319,** 303–305.

MATSUI, T., AND Y. ABE 1986b. Impact-induced atmospheres and oceans on Earth and Venus. *Nature* **322,** 526–528.

MCCLATCHEY, R. A., R. W. FENN, J. E. A. SELBY, F. E. VOLZ, AND J. S. GARING 1971. *Optical Properties of the Atmosphere*. Tech. Report., AFCRL-71-0279, Bedford, MA.

MIHALAS, D. 1978. *Stellar Atmospheres*, 2nd ed. Freeman, San Francisco.

MOORE, C. E., M. G. J. MINNAERT, AND J. HOUTGAST 1966. *The Solar Spectrum 2935 A to 8770 A: Second Revision of Rowland's Preliminary Table of Solar Spectrum Wavelengths.* Nat. Bur. Stand. Monogr. No. 61, U.S. Govt. Printing Office, Washington, DC.

NEWMAN, M. J., AND R. T. ROOD 1977. Implications of solar evolution for the Earth's early atmosphere. *Science* **198**, 1035–1037.

POLLACK, J. B. 1971. A nongrey calculation of the runaway greenhouse: Implications for Venus' past and present. *Icarus* **14**, 295–306.

ROBERTS, R. E., J. E. A. SELBY, AND L. M. BIBERMAN 1976. Infrared continuum absorption by atmospheric water vapor in the 8–12 μm window. *Appl. Opt.* **15**, 2085–2090.

SAFRONOV, V. S. 1972. *Evolution of the Protoplanetary Cloud and Formation of the Earth and Planets.* NASA Tech. Transl., TTF-677.

SMITH, H. J. P., D. J. DUBE, M. E. GARDNER, S. A. CLOUGH, F. X. KNEIZYS, AND L. S. ROTHMAN 1978. *FASCODE—Fast Atmospheric Signature Code (Spectral Transmittance and Radiance).* AFGL-TR-78-0081, Air Force Geophysics Laboratory, Hanscom AFB, MA.

TOMASI, C. 1979a. Non-selective absorption by atmospheric water vapour at visible and near infrared wavelengths. *Quart. J. R. Meteor. Soc.* **105**, 1027–1040.

TOMASI, C. 1979b. Weak absorption by atmospheric water vapor in the visible and near-infra-red spectral region. *Il Nuovo Cimeto* **2**, 511–526.

TOON, O. B., AND J. B. POLLACK 1976. A global average model of atmospheric aerosols for radiative transfer calculations. *J. Appl. Meteor.* **15**, 225–246.

VARDAVAS, I. M., AND J. H. CARVER 1984. Solar and terrestrial parameterizations for radiative-convective models. *Planet. Space Sci.* **32**, 1307–1325.

VARDAVAS, I. M., AND J. H. CARVER 1985. Atmospheric temperature response to variations in CO_2 concentration and the solar-constant. *Planet. Space Sci.* **33**, 1187–1207.

WALKER, J. C. G., P. B. HAYS, AND J. F. KASTING 1981. A negative feedback mechanism for the long-term stabilization of Earth's surface temperature. *J. Geophys. Res.* **86**, 9776–9782.

WATSON, A. J., T. M. DONAHUE, AND W. R. KUHN 1984. Temperatures in a runaway greenhouse on the evolving Venus: Implications for water loss. *Earth Planet. Sci. Lett.* **68**, 1–6.

WETHERILL, G. W. 1985. Occurrence of giant impacts during the growth of the terrestrial planets. *Science* **228**, 877–879.

ZAHNLE, K. J., AND J. F. KASTING 1986. Mass fractionation during transsonic escape and implications for loss of water from Mars and Venus. *Icarus* **68**, 462–480.

ZAHNLE, K. J., J. F. KASTING, AND J. B. POLLACK 1988. Evolution of a steam atmosphere during the Earth's accretion. *Icarus* **74**, 62–97.